Journal of Astronomical Telescopes, Instruments, and Systems

AstronomicalTelescopes.SPIEDigitalLibrary.org

Advanced ultraviolet, optical, and infrared mirror technology development for very large space telescopes

H. Philip Stahl

SPIE.

H. Philip Stahl, "Advanced ultraviolet, optical, and infrared mirror technology development for very large space telescopes," *J. Astron. Telesc. Instrum. Syst.* **6**(2), 025001 (2020), doi: 10.1117/1.JATIS.6.2.025001

Advanced ultraviolet, optical, and infrared mirror technology development for very large space telescopes

H. Philip Stahl*
NASA Marshall Space Flight Center, Huntsville, Alabama, United States

Abstract. The Advanced Mirror Technology Development (AMTD) project was a 6-year effort to mature technologies required to enable 4-m-or-larger monolithic or segmented ultraviolet/optical/infrared space-telescope primary-mirror assemblies for general astrophysics and exoplanet missions. AMTD used a science-driven systems-engineering approach. Starting with science requirements, engineering specifications were derived for the primary mirror aperture diameter, areal density, surface error, and stability. The most impactful specification may be 10 pm per 10-min wavefront stability. Advances were made to six key technologies: (1) fabricating large-aperture low-areal-density high-stiffness mirror substrates; (2) designing support systems; (3) correcting mid/high-spatial frequency figure error; (4) mitigating segment edge diffraction; (5) phasing segment-to-segment gaps; and (6) validating integrated models. AMTD successfully demonstrated a process to make substrates as large as 1.5 m and as thick as 40 cm by stacking multiple core elements and low-temperature fusing them together. To help predict on-orbit performance and assist in architecture trade studies, integrated models were created for two mirror assemblies (1.5-m Ultra-Low-Expansion (ULE®) mirror fabricated by AMTD partner Harris Corp. and 1.2-m Zerodur® mirror owned by Schott North American). X-ray-computed tomography was used to construct the 1.5-m ULE® mirror's "as-built" model. These models were validated by testing full- and subscale components in relevant thermovacuum environments.
 [DOI: 10.1117/1.JATIS.6.2.025001]

Keywords: space telescope; mirror technology; manufacturing techniques; integrated modeling.

Paper 19133 received Dec. 31, 2019; accepted for publication May 6, 2020; published online May 23, 2020.

1 Introduction

The Advanced Mirror Technology Development (AMTD) project was a 6-year effort initiated in fiscal year 2012 to mature the technology readiness level (TRL) of critical technologies required to enable 4-m-or-larger monolithic or segmented ultraviolet, optical, and infrared (UVOIR) space-telescope primary-mirror assemblies for general astrophysics and ultra-high-contrast observations for exoplanet missions. The study was conducted by an integrated team of government and industry scientists, systems engineers, and technologists listed in the acknowledgements.

AMTD used a science-driven systems-engineering approach. Starting with science requirements, AMTD derived engineering specifications for the primary mirror aperture diameter, mirror areal density, surface error, and stability. The most impactful specification defined by AMTD may be 10 pm per 10-min wavefront stability. To accomplish its trade studies, AMTD developed four design and modeling tools: Arnold Mirror Modeler (AMM), sensitivity and performance evaluator for coronagraph leakage (SPECL), thermal modulation transfer function (T-MTF), and Fast Response Simulator for Telescopes (FaRSiTe).

AMTD matured technologies and specifications, documented lessons learned, and identified new areas of investigation for six enabling technologies:

- large-aperture, low-areal density, high-stiffness mirror substrates;
- support system;

*Address all correspondence to H. Philip Stahl, E-mail: h.philip.stahl@nasa.gov

- mid/high-spatial frequency figure error;
- segment edges;
- segment-to-segment gap phasing;
- integrated model validation.

AMTD successfully demonstrated the utility of stacked-core technology to enable ultrastiff/ultrastable substrates. This was accomplished by demonstrating three specific capabilities: (1) the ability to low-temperature-fuse (LTF) stack cores with strength greater than the design allowable limit; (2) the ability to make mirror substrates as thick as 40 cm; and (3) the ability to laterally scale the stacked-core technique to a 1.5-m diameter by 165-mm thick, 450-Hz mirror (1/3 scale of a 4-m mirror). Additionally, AMTD documented lessons learned regarding low-temperature-slumping (LTS) of large stiff mirror substrates.

To help predict on-orbit performance and assist in architecture trade studies, the engineering team developed integrated structural, thermal, and optical performance (STOP) models of candidate mirror assembly systems, including substrates, structures, and mechanisms. These models were validated by testing full- and subscale components in relevant thermovacuum environments. AMTD characterized the mechanical and thermal performance of a 40-cm diameter by 40-cm thick section of a 4-m Ultra-Low-Expansion (ULE®) glass mirror, a 1.5-m diameter ULE® mirror, and a 1.2-m Extremely Lightweight Zerodur® mirror (ELZM) (owned by Schott North American). AMTD correlated the measured data with predictions from "as-built" integrated STOP models. X-ray-computed tomography was used to construct the 1.5-m ULE® glass mirror as-built model. Additionally, AMTD performed a thermal test of a mirror strut mount interface traceable to the Wide Field Infrared Survey Telescope (WFIRST).

This survey paper summarizes 6 years of work,[1–6] the results of which are documented more fully in the references cited within each section. Section 2 reviews the background relevance for the study (i.e., what science is enabled by the technology developed). Section 3 defines the goals and objectives of the study (i.e., the technologies matured in phase 1 and phase 2) and the study's methodology. Section 4 describes how the engineering specifications that the technology needed to achieve were derived using the science-driven systems-engineering methodology. Section 5 summarizes AMTD's accomplishments for each of the six key technology areas. Finally, Sec. 6 assesses the TRL advances achieved by AMTD.

2 Background

"Are we alone in the Universe?" is probably the most compelling science question of our generation. Per the 2010 *New Worlds, New Horizons* decadal report,[7] "One of the fastest growing and most exciting fields in astrophysics is the study of planets beyond our solar system. The ultimate goal is to image rocky planets that lie in the habitable zone of nearby stars."

Also, per the decadal, "An advanced, large-aperture UVOIR telescope is required to enable the next generation of compelling astrophysics and exoplanet science," because UVOIR measurements provide robust, often unique diagnostics for investigating astronomical environments and objects. UVOIR observations are responsible for much of our current astrophysics knowledge and will produce as-yet unimagined paradigm-shifting discoveries—helping to answer fundamental questions, such as: How do galaxies assemble their stellar populations? How do galaxies and the intergalactic medium interact? How did planets and smaller bodies in our solar system form and evolve?

Therefore, the decadal recommended, as its highest priority, a medium-scale activity, such as a "New Worlds Technology Development Program," to "lay the technical and scientific foundations for a future space imaging and spectroscopy mission." The National Research Council report *NASA Space Technology Roadmaps and Priorities*[8] states that the second-highest technical challenge for NASA, regarding expanding our understanding of Earth and the universe in which we live, is to "develop a new generation of astronomical telescopes that enable discovery of habitable planets, facilitate advances in solar physics, and enable the study of faint structures around bright objects by developing high-contrast imaging and spectroscopic technologies to provide unprecedented sensitivity, field of view, and spectroscopy of faint objects." NASA's

Enduring Quests, Daring Visions[9] called for a Large UV-Optical-Infrared (LUVOIR) Surveyor Mission to "enable ultra-high-contrast spectroscopic studies to directly measure oxygen, water vapor, and other molecules in the atmospheres of exoEarths" and "decode the galaxy assembly histories through detailed archeology of their present structure." As a result, NASA will study in detail a LUVOIR surveyor and a HabEx Imager concept for the 2020 decadal survey.[10] Additionally, AURA's *From Cosmic Birth to Living Earths*[11] details the potential revolutionary science that could be accomplished from "directly finding habitable planets showing signs of life."

Direct imaging and characterization of habitable planets requires a large-aperture telescope with an extremely smooth and stable primary mirror surface. For an internal coronagraph, this requires correcting wavefront errors (WFEs) via one or more deformable mirrors (DMs) and keeping that correction stable to a few pm rms for the duration of the science observation. This places severe specification constraints upon the performance of the observatory, telescope, and primary mirror. The smoother the primary mirror surface is, the easier it is for the DM to produce a dark hole. Yet, the real problem is stability. Dynamic WFE introduces speckle noise, which can mask a planet detection. Although dynamic WFE can arise from both mechanical and thermal sources, the focus of AMTD is understanding how to affordably make stiff mechanical-stable mirrors. For either large monolithic mirrors or smaller mirror segments, mechanical disturbances create rigid-body motion of the mirror on its mount. These inertial motions introduce dynamic WFE when the mirror distorts (or bends) as it reacts against its mount. Achieving wavefront stability is a systems-engineering trade between mirror assembly stiffness (substrate and mount) and vibration isolation. In Ref. 12, WFE is proportional to the rms magnitude of the applied inertial acceleration divided by the square of the structure's first mode frequency. Therefore, to achieve ultrastability requires either a very stiff system or very low acceleration loads.

Finally, the decadal also recommended a NASA Core Research Program UVOIR Capability investment because, while compelling, a 4-m-diameter aperture UVOIR telescope requires further technology development. As a result, the NASA Office of the Chief Technologist's Science Instruments, Observatory, and Sensor Systems Technology Assessment Roadmap states that technology to enable a future UVOIR or high-contrast exoplanet mission needs to be at TRL-6 by 2018, so a viable flight mission can be proposed to the 2020 decadal survey.[2,13]

3 Objectives and Methodology

AMTD's objective was to mature toward TRL-6 the critical technologies necessary to enable both large monolithic and segmented ultrastable UVOIR space telescopes. Phase 1 advanced the technology readiness of six key technologies required to make an integrated primary mirror assembly (PMA) for a large-aperture UVOIR space telescope:

- large-aperture, low-areal density, high-stiffness mirror substrates;
- support system;
- mid/high-spatial frequency figure error;
- segment edges;
- segment-to-segment gap phasing;
- integrated model validation.

Phase 2 continued development on three of these key technologies:

- large-aperture, low-areal density, high-stiffness mirror substrates;
- support system;
- integrated model validation.

AMTD accomplished its objectives using a science-driven systems-engineering approach that depended on collaboration between a Science Advisory Team and a Systems Engineering Team. The Science Advisory Team provided AMTD with advice from experts in the area of

UVOIR astrophysics, exoplanet characterization, and terrestrial and space telescope performance requirements. The Engineering Team provided expertise in the design, fabrication, and testing of monolithic and segmented, large-aperture ground and UVOIR space telescopes. The two teams worked collaboratively to ensure that AMTD matured technologies required to enable the highest priority science and result in a high-performance, low-cost, low-risk system. The names of all those involved in AMTD are listed in the acknowledgements section.

The responsibilities of the Science and Engineering teams were as follows.

- To derive engineering specifications for monolithic and segmented-aperture, normal-incidence mirrors, which flow down from the on-orbit performance needed to enable the required astrophysical measurements and flow up from implementation constraints.
- To identify the technical challenges in meeting these engineering specifications.
- To iterate between the science needs and engineering specifications to mitigate challenges.
- To prioritize technology development to yield the best on-orbit performance for the lowest cost and risk.

To help predict on-orbit performance and assist in architecture trade studies, the engineering team developed STOP models of candidate mirror assembly systems, including substrates, structures, and mechanisms. These models were validated by tests of full- and subscale components in relevant thermovacuum environments.

4 Science-Driven Systems Engineering

The purpose of AMTD was not to design a telescope for a particular mission or to work with a specific instrument. Rather, its purpose was to produce a set of PMA engineering specifications that defines the on-orbit telescope performance required to enable the desired science and to develop the technology necessary to achieve those specifications. AMTD's philosophy was to define a set of specifications that enveloped the most demanding requirements of all potential science. If the PMA meets these specifications, it should work with most potential science instruments. Defining mirror coating or contamination specifications was beyond the scope of AMTD.

Both general astrophysics and exoplanet science contributed performance requirements, such as sensitivity, signal to noise, diffraction limited performance, encircled energy, and point spread function (PSF) stability. These flowed directly into aperture size and WFE specifications for potential telescope assemblies. Additional specifications were obtained by applying mass and volume capacities of current and planned launch vehicles. Accomplishing NASA's highest priority in astrophysics science (such as ultra-high-contrast imaging to characterize exoplanets) requires optical telescope assemblies (OTAs) and primary mirror assemblies with never-before-required performance specifications.

Starting with science requirements, engineering specifications were derived for the primary mirror aperture diameter, primary mirror areal density, rms surface figure error (SFE) for a monolithic or segmented primary mirror, primary mirror SFE power spectral density, and WFE stability.[14,15] The WFE budget is divided into specifications that drive structural, thermal, and optical design. Using integrated STOP models of candidate PMAs (including substrates, structures, and mechanisms) and complete OTAs, architectural design trades were performed as assessed for their ability to meet the performance requirements. For this analysis, AMTD used existing commercial tools (NASTRAN, ANSYS, Sigmadyne, SigFit, Thermal Desk Top, etc.) and developed new design and modeling tools: AMM,[16,17] SPECL,[18] T-MTF,[19] and FaRSiTe.[2] Details of these four tools can be found in Sec. 8.

4.1 *Primary Mirror Physical Specifications*

The AMTD Science Advisory Team specified that the minimum aperture diameter of interest was 4 m and that larger was better. A key specification derived from aperture diameter is areal density. Table 1 shows one potential allocation for the maximum mass of the primary mirror as a function of the mission's launch vehicle and its resulting areal density. Note that current

Table 1 Maximum mass allocation as a function of launch vehicle.[25]

Launch vehicle	Delta-IVH	Block-1B	Block-2 min	Block-2 max
Payload mass to SE-L2 with 43% margin (kg)	7000	24,500	31,500	38,500
Spacecraft allocation (kg)	2400	4500	6500	8500
Observatory allocation (kg)	4600	20,000	25,000	30,000
Science instruments (kg)	1600	2000	2500	3000
Telescope (PMA, SMA, and structure) (kg)	3000	18,000	22,500	27,000
SMA and structure (kg)	1000	6000	6500	7000
PMA allocation (kg)	2000	12,000	16,000	20,000
Primary mirror allocation (kg)	1000	6000	8000	10,000
Primary mirror areal mass (kg/m^2)				
4-m diameter (12.5 m^2)	80	480	640	800
8-m diameter (50 m^2)	20	120	160	200
12-m diameter (100 m^2)	10	60	80	100
16-m diameter (200 m^2)	5	30	40	50

state-of-the-art areal density for UVOIR glass primary mirror assemblies is 35 kg/m^2 and state-of-the-practice is 50 kg/m^2.[20,21] The PSF of various segmentation architectures is another implication of aperture diameter that AMTD investigated as it relates to the coronagraph inner working angle (IWA).[15,22–24]

Derived from a desired telescope diffraction-limited performance of 500 nm, a nominal 7 nm rms specification was defined for the primary mirror's SFE. This error was partitioned between low-, mid-, and high-spatial frequencies (Table 2) based on what is required to enable the creation of the coronagraph "dark hole" and minimize leakage into the dark hole from uncorrectable spatial figure errors. It is assumed that a DM will be used to create the dark hole and that it can correct errors up to 30 cycles per diameter. Therefore, to prevent leakage into the dark hole, the primary mirror must be smooth up to 90 cycles—because uncorrectable errors up to 90 cycles can "alias" energy into the dark hole. Finally, note that in Table 2 segmented mirrors have a smaller error specification. This is because, for a segmented mirror, error must be allocated to aligning and co-phasing the individual segments to each other to form an equivalent "monolithic" primary mirror. As shown in Table 2, AMTD assumed that segment co-phasing

Table 2 Primary mirror SFE as a function of spatial frequency.

	Monolithic	Segmented
Total SFE (nm rms)	7	7
Figure/low-spatial (<4 cycles per diameter) (nm rms)	5	3.5
Mid-spatial (4 to 60 cycles per diameter) (nm rms)	5	3.5
Segment to segment phasing error (nm rms)	0	5
High-spatial (60 cycles to 10-mm period) (nm rms)	1	0.7
Roughness (<10-mm period) (nm rms)	0.3	0.2

could be achieved at a 5-nm-rms precision. If better co-phasing can be achieved, then the fabrication error allocations can be increased.

4.2 *Primary Mirror Stability Specification*

A fundamental tenet of systems engineering is the ability to decompose a system into its constituent parts to specify, in this case, the optical telescope performance independent of the science instruments. To do this for exoplanet science requires modeling and analyzing the telescope and coronagraph as an integrated system. Depending on a given coronagraph's sensitivity, small dynamic perturbations of the input wavefront can produce speckles in the dark hole—contrast leakage—that might obscure a planet or lead to a false positive. The key challenge is understanding how to create a wavefront dynamic stability specification for the primary mirror. To this end, AMTD developed a series of increasingly sophisticated modeling tools to estimate the contrast leakage that occurs when dynamically aberrated wavefronts are propagated through candidate coronagraphs.[18,22–24]

A summary finding of this study is that, to prevent unwanted contrast leakage into the dark hole, the telescope wavefront must be stable to better than 10 pm rms per 10 min.[14] However, this specification is poetry. The actual specified maximum WFE amplitude depends on the spatial frequency of the error.[4,5,18,23,24] And, the actual specified time period is wavefront control cycle, which, depending on the size of the telescope aperture and the brightness of the target star, can vary from a few minutes to >20 min.

For example, Table 3 shows the sensitivity of a coronagraph published by N'Diaye[26] for use on a segmented aperture telescope similar to the James Webb Space Telescope with an IWA of $4.5\lambda/D$. In general, segment level errors are more important than global aberrations because segment level errors produce speckles at the same spatial frequency as the dark hole. For this system, global errors produce speckles that are inside the IWA. At the IWA, segment piston and tip/tilt errors are the most important because this is where their speckles are located. Higher order segment level errors (power, astigmatism, and trefoil) are less important at the IWA because, since they are higher spatial frequency errors, their speckles occur further into the dark hole. To illustrate the use of this analysis, if the primary mirror was the only error source in the telescope, then its SFE specification would be one half of the values in Table 3.

Table 3 Maximum random aberration amplitude as a function of contrast leakage.

ROI = 4.5 to 5.5λ/D	Aberration	PV WFE (pm) for 1×10^{-10} photometric noise	PV WFE (pm) for 5×10^{-11} systematic noise
Segment errors	Piston	670	29
	Tip/tilt	230	26
	Power	1200	130
	Astigmatism	1900	190
	Trefoil	11,000	330
Global errors	Power	22,000	22,000
	Spherical	24,000	9600
	Coma	69,000	55,000
	Trefoil	62,000	12,000
	Hexafoil	120,000	12,000
Back plane	Bend About X	1500	330

5 Technology Development Accomplishments

AMTD matured (toward TRL-6) six key technologies necessary to enable large monolithic or segmented UVOIR space telescopes: large-aperture, low-areal density, high-stiffness mirror substrates; support system; mid/high-spatial frequency figure error; segment edges; segment-to-segment gap phasing; and integrated model validation.

It was necessary to make progress on these technologies simultaneously because they are all required to make an integrated PMA that has sufficient on-orbit performance to enable the required science measurements. Moreover, most of them are related to stiffness. The primary emphasis of AMTD was to develop and demonstrate a cost-effective process to manufacture high-stiffness low-mass large aperture mirror substrates. The reason for this emphasis is that on-orbit performance is largely driven by mirror stiffness. However, total PMA stiffness also depends on substrate and support design. Also related to substrate stiffness is the ability to eliminate mid/high-spatial figure errors and polishing edges.

5.1 *Large-Aperture, Low-Areal Density, High-Stiffness Mirror Substrates*

Whether the PMA is monolithic or segmented, low-areal density high-stiffness substrates are an enabling technology. The easiest way to increase stiffness is to make the substrate thicker. Before AMTD, the state of the art for ULE® mirrors was defined by the Advanced Mirror System Demonstrator (AMSD) and WFIRST. Both of these mirrors have a first mode frequency of ~200 Hz. The AMSD mirror is 1.4 m × 0.06 m, 10 kg/m^2 and was manufactured as a three-layer substrate (face/back sheet and core) via a LTF/LTS process. The WFIRST primary mirror is 2.4 m × 0.2 m, 50 kg/m^2 and was fabricated via LTF using curved components. At 21-cm thick, the WFIRST primary mirror represents the current state of the art for monolithic mirrors. This thickness is limited by Harris Corp's ability to abrasive water jet (AWJ) cut core structures. By comparison, Schott AG has a maximum core machining depth of 28 cm.

AMTD partner Harris Corp. successfully matured the technology for low-areal density high-stiffness substrates by demonstrating a 5-layer, 4-cm-thick mirror manufactured via the new "stacked and fuse" process. To make thicker mirrors, multiple core elements were cut [Fig. 1(a)] and stacked between a face sheet and back sheet, then LTF'd together into a plano/plano substrate. The substrate was then LTS'd to a radius of curvature. Using this new process, a 43-cm diameter "cut-out" of a 4-m diameter, 40-cm-thick, <45 kg/m^2 mirror substrate was fabricated [Fig. 1(b)]. Harris Corp estimated that this process significantly reduces the cost to fabricate mirrors, possibly by as much as 30%.[27,28]

In AMTD phase 1, Harris Corp tested the core-to-core LTF bond strength using 12 modulus of rupture (MOR) test articles (Fig. 2). Also in phase 2, Harris performed an A-basis test of the core-to-core LTF bond strength as a function of alignment using 60 MOR samples: 30 samples were assembled with nominal alignment and 30 samples were deliberately misaligned. Based on 49 of the samples, the A-basis Weibull 99% confidence strength allowable was found to be 17.5 MPa, which is ~50% higher than the most conservative design allowable value for margin of safety calculations at the core-to-plate LTF bond. The data on the 50 samples ranged from 60% to 250% above this design allowable value.[2]

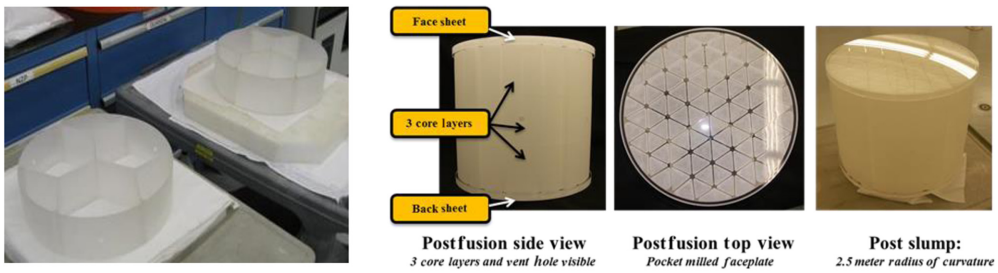

Fig. 1 A 43-cm diameter × 40-cm-thick mirror was manufactured by (a) fabricating individual core elements that were (b) stacked, fused to a plano/plano, and slumped to a 2.5-m radius.

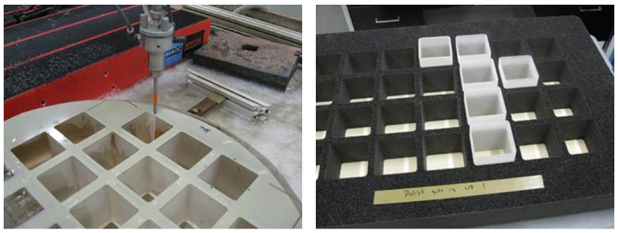

(a) (b)

Fig. 2 MOR test article fabrication: (a) in AWJ and (b) post-AWJ.

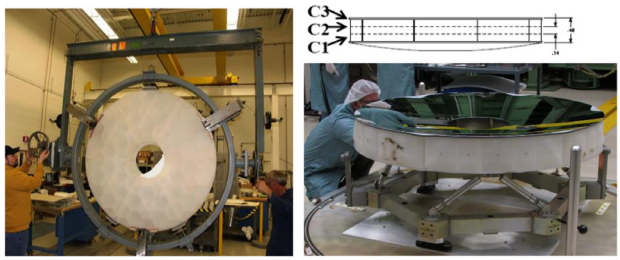

(a) (b)

Fig. 3 (a) LTF mirror substrate; (b, top) five-layer design; and (b, bottom) completed mirror assembly.

To demonstrate lateral scalability, Harris Corp. used the "stack and fuse" process to manufacture a 1.5 m × 165 mm, 5-layer, 400-Hz first mode mirror. This was a major milestone for AMTD phase 2. The reason that this mirror has three core element layers instead of one is because it is a subscale version of a 5-layer, 4 m × 440 mm mirror in which each core element layer is 150-mm thick. The mirror consisted of a face sheet, back sheet, and 18 core elements (6 elements per core layer), which were first fused together to form a planar substrate [Fig. 3(a)]. The substrate was then slumped to a 3.5-m radius of curvature [Fig. 3(b)]. Note that this radius was selected because a slumping body was available. Also note that a single-core layer version of this 400-Hz mirror would meet the performance needs for a 12- to-16-m segmented aperture telescope.[29,30]

During AMTD-1, when the 43-cm deep-core mirror was slumped from a 5- to 2.5-m radius of curvature, there was noticeable deformation in the core walls. To quantify the magnitude of this bending, MSFC imaged the mirror's internal structure via x-ray tomography. A small amount of bending was expected because slumping places the concave surface in compression and stretches the convex surface; this places the core elements in shear stress. To mitigate this effect, the design of the 1.5-m mirror was adjusted to increase the gap between core elements. The measured deformation exceeded that expectation. Fortunately, analysis indicated that such core-wall bending had a limited effect on the mirror's strength. Using this lesson learned in designing the 1.5-m 1/3 scale model of a 4-m mirror, Harris Corp. used proprietary modeling tools to predict the viscoelastic performance of the mirror [Fig. 4(a)]. The spacing between the wedge-shaped core elements was specifically increased to prevent adjacent core walls from

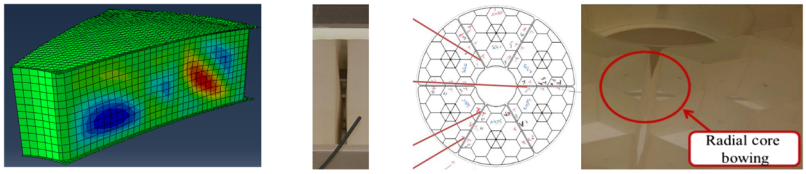

(a) (b)

Fig. 4 (a) Predicted viscoelastic deformation used to design mirror substrate; (b, three images) actual viscoelastic deformation; four-locations had gaps of <0.25 mm.

touching. Unfortunately, because of a fixture issue from an external vendor, when the mirror was assembled, some of the core elements were shifted toward the center of the mirror by up to 20 mm, reducing the gap size. As a result, when the core walls bent, they contacted in one location (but did not fuse) and got within <0.25 mm at three other locations [Fig. 4(b)]. MSFC imaged the internal structure of the mirror via x-ray-computed tomography and used that data to create an as-built 3-D model of the mirror to predict its mechanical and thermal performance.[5]

Core-wall bending is complicated. Previous to AMTD, the only mirrors fabricated via the LTF/LTS process were AMSD and Multiple Mirror Segment Demonstrator, neither of which exhibited core-wall bending. Preliminary analysis indicates that the effect depends on shear stress in the core. The greater the amount of shear stress is, the greater the amount of viscous flow of the glass during LTS is, and the greater the core-wall bending is. Preliminary analysis indicates that this shear stress is proportional to the unsupported radial core-wall length divided by the radius of curvature (independent of core thickness and whether the core is composed of a single layer or multiple layers). The AMTD-1 mirror (2.5-m ROC, 0.43-m diameter × 400-mm thick) had significantly larger core cells than the AMTD-2 mirror (3.5-m ROC, 1.5-m diameter × 165-mm thick) and thus less bending. If the 1.5-m mirror had been LTS'd to a 7.5-m ROC, it likely would have had negligible bending.

5.2 *Support System*

Large-aperture mirrors require large support systems to ensure that they survive launch and deploy on-orbit in a stress-free and undistorted shape. Additionally, segmented mirrors require large structure systems that establish and maintain the mirror's shape relative to the back plane.

AMTD used the AMM to design strut and launch support systems for candidate open- and closed-back 4-m class monolithic mirrors. Dozens of point designs were generated.[31–34] Additionally, AMM was used to investigate the stiffness of candidate 4-m class mirror designs for a nominal 720-kg mass constrained mission (i.e., launched via Delta-IV Heavy), as shown in Table 4, and mass relaxed designs enabled by the Space Launch System (Table 5). Dynamic and static analysis was performed on candidate mirrors to determine stress on internal structural elements and at the mount interfaces during launch. Several launch support system configurations were identified that keep internal stress below 600 psi (Fig. 5).

Dynamic WFE is particularly important for coronagraphy. Dynamic WFE at levels >10 pm per control cycle can introduce speckle noise that can degrade exoplanet science. An important dynamic WFE is inertial deformation. Inertial WFE is produced when a mirror is accelerated by a mechanical disturbance, causing it to react (i.e., bend) against its mounts. Its simplest example is gravity sag. The acceleration of gravity causes a mirror to bend on its mount. On-orbit,

Table 4 4-m mirror point designs (with thin face sheets).

Architecture	Solid	Closed back				
Mass (kg)	716	512	590	660	700	841
Thickness (mm)	26.5	315	415	420	515	526
Free–free first mode (Hz)	9.8	101	115	123	136	145

Table 5 4-m closed-back mirror point designs (with thicker face sheets).

Thickness (m)	0.40	0.45	0.6	0.75
Mass (kg)	900	2200	2560	2860
Free–free first mode (Hz)	100	180	215	245

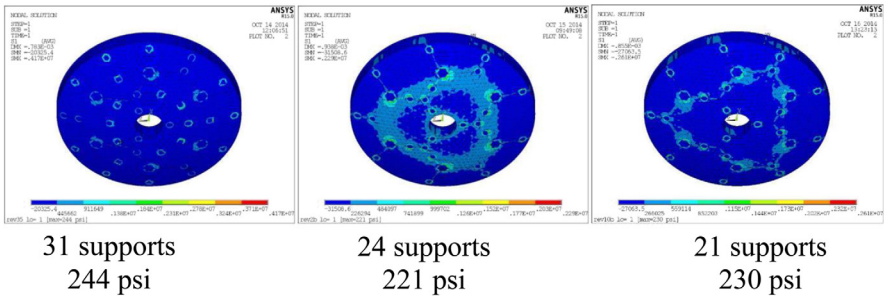

Fig. 5 Potential launch support designs evaluated for stress distribution.

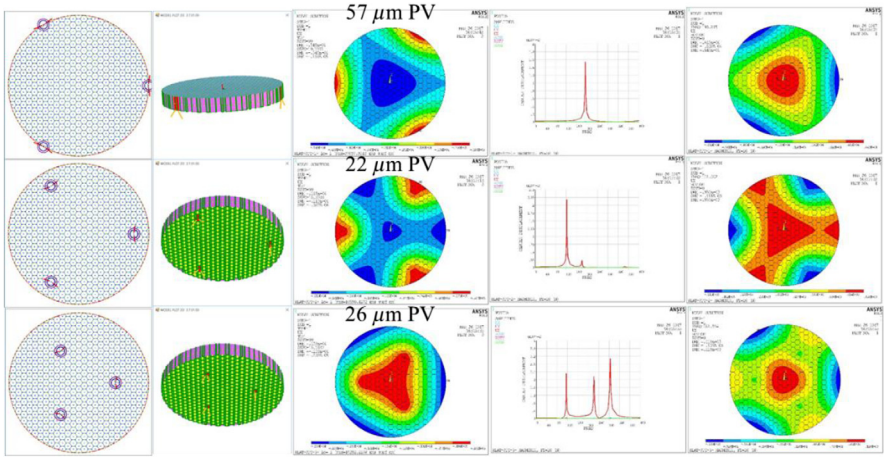

Fig. 6 Static gravity sag and dynamic deformation of 180-Hz, 4-m diameter closed-back mirror on 3-point mount attached at edge, 80% and 50% radial locations. The first two columns show the mirror mount locations. The third column is the 1-G gravity sag for the mirror on its mount. The fourth column shows the resonant response of the mount system. It is at these frequencies that the mirror experiences its maximum acceleration and thus its maximum inertia deformation. The last column illustrates how the inertial deformation shape matches the mirror's 1-G sag.

assuming that no resonant mode is excited, a mirror's inertial WFE has the same shape as its gravity sag with an amplitude proportional to the disturbance's "G-acceleration." AMTD studied inertial WFE for various mirror substrates on both 3-, 6-, 9-, and 18-point mounts and mounts attached to the substrate at the edge, 80% and 50% radial points (Fig. 6).[32,33,35] As to which mount configuration might be best, it depends on the application. The optimum configuration for an imaging application might be different from that for coronagraphy. For example, where to locate the mounts radially depends on the coronagraph's sensitivity to power. Moreover, whether to use 3 or 6 mount points depends on its sensitivity to trefoil versus hexafoil.

5.3 *Mid/High-Spatial Frequency Figure Error*

High-contrast imaging requires mirrors with very smooth surfaces (<10 nm rms). Although DMs can correct low-order errors, they cannot correct mid- and high-spatial frequency errors caused by the fabrication process or coefficient of thermal expansion (CTE) inhomogeneity. These errors are important because they can introduce artifacts into the dark hole.

AMTD partner Harris Corp. specifically designed the 43-cm deep-core mirror to have a pocketed face sheet to minimize the mid/high-spatial frequency quilting error from polishing pressure and thermal stress. However, as expected because the face sheet was thin, the 43-cm mirror did have quilting associated with the pocketing. Harris removed this quilting via ion

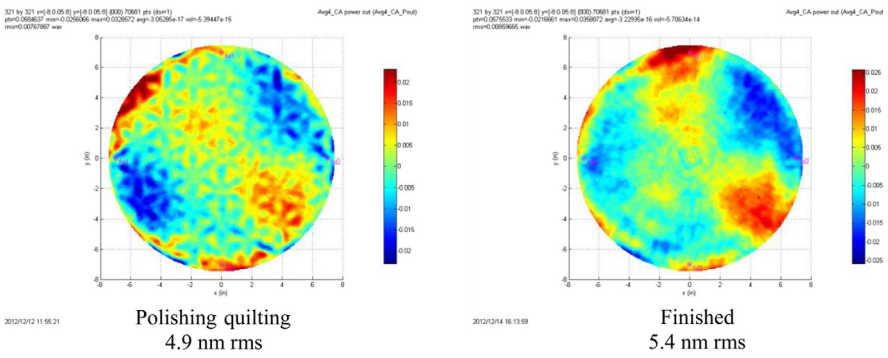

Fig. 7 Harris Corp ion-polished the AMTD 43-cm to remove cell quilting, resulting in a 5.4-nm-rms surface.

polishing to produce a mirror with a 5.4-nm-rms finished surface (Fig. 7). AMTD assesses the ability to correct mid-spatial errors to be demonstrated (i.e., TRL-6).

Because on-orbit temperature can be different from the fabrication temperature, thermal stress, even for a low-CTE material such as ULE® glass, can cause SFEs. To understand the impact of thermal deformation, it must be quantified. MSFC tested the 43-cm and 1.5-m ULE® mirrors and a 1.2-m Zerodur® mirror from 230 to 300 K (Figs. 8 and 9).[36,37]

As shown in Fig. 10, the cryodeformation of the 43-cm mirror exhibits no quilting signature similar to the pattern seen in Fig. 7. Its mid-spatial frequency error was <4 nm rms.[36] Similarly, the Schott 1.2-m Zerodur® mirror also displays no thermal-induced cryodeformation associated with its machined isogrid core structure (Fig. 11). Note that the fringe-shaped pattern is an artifact of the measurement algorithm because the mirror was only polished to about 100 nm rms to save money. By comparison, because the 1.5-m ULE® mirror does not have a pocketed face sheet, it is not expected to have quilting. However, as shown in Fig. 12, its cryo-deformation does contain a mid-spatial frequency error which is correlation to the mirror's core pattern.

There are several important lessons to be learned from Figs. 11 and 12. First, the spatial frequency of the cryodeformation for the Zerodur® and ULE® mirrors is different. Moreover,

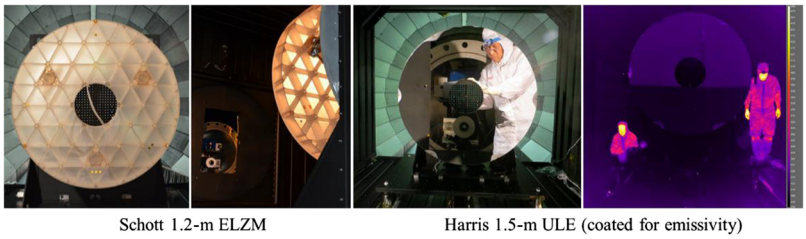

Fig. 8 Schott 1.2-m ELZM and Harris 1.5-m ULE® mirrors under test in XRCF.

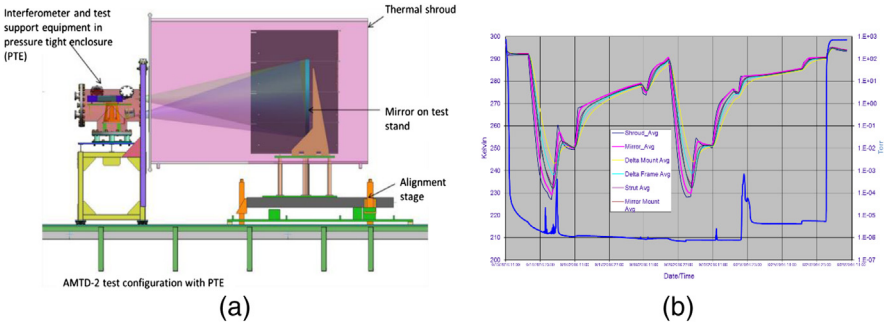

Fig. 9 XRCF thermal characterization: (a) test setup and (b) typical thermal profile.

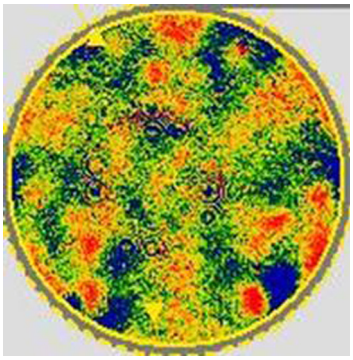

Fig. 10 43-cm mirror 253- to 293-K cryo-deformation mid-spatial error is <4 nm rms and shows no quilting pattern.

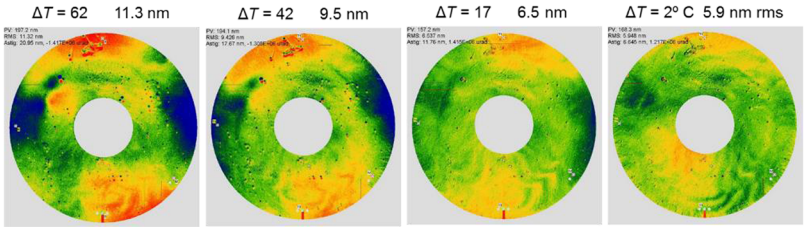

Fig. 11 1.2-m Zerodur® mirror's cryodeformation shows no correlation with core pattern.[38]

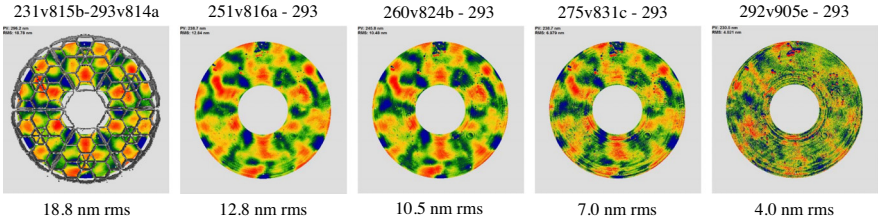

Fig. 12 1.5-m ULE® mirror's cryodeformation has mid-spatial error, after removal of 36 Zernike terms, which increases with temperature change and, as shown in the left image, is correlated with the core.

if uncorrected, their impact will be different. The ULE® mirror has more mid-spatial frequency content than the Zerodur® mirror. Fortunately, both deformations are in the capture range for state-of-practice computer-controlled polishing processes. Thus both could be corrected to the specified surface figure necessary to enable high-contrast imaging at a specific temperature. Second, the temperature sensitivity of both mirrors is similar. The Zerodur® mirror has ~0.2 nm/K of surface deformation, and the ULE® mirror has ~0.3 nm/K. This is important because it places a constraint on the thermal stability specification for the mirror. For example, if the coronagraph that will be paired with the ULE® mirror requires that the amplitude of the surface thermal deformation be <0.003 nm, then the temperature of the mirror must be stable to <10 mK.

Finally, in support of the WFIRST program, the 1.5-m ULE® mirror was soak tested at 260 K for 12 days to assess the AMTD mirror mount interface's thermal stability for potential use on WFIRST. The test indicated that the AMTD mirror mount design, which was designed to be athermal at 250 K, was stable within the metrology uncertainty, and there was no indication of mount effects printing through to the surface.

5.4 *Segment Edges*

For a segmented primary mirror, the edge diffraction and the quality of segment edges impacts the telescope's PSF, contributes to stray light noise, and affects the total collecting aperture.[39,40] All of these impact high-contrast imaging. One mitigation for these effects is edge apodization.

AMTD partner STScI successfully demonstrated an achromatic apodization coating. A glass grayscale prototype mask was fabricated using chromium microdots and tested at the Brookhaven National Laboratory beam line. When used at high $F/\#$, the synchrotron beam simulates collimated starlight. The purpose of the test is to use a Fourier transform spectrometer to measure the mask's transmission (to an accuracy of ~0.1%) from 500 to 1000 nm (Fig. 13). The coating provides a variable attenuation with uniform performance over a broad spectral band. Such a coating deposited on a segmented mirror enables a high-contrast imaging PSF by minimizing edge diffraction, straylight, and structure obscuration diffraction.[41]

5.5 *Segment-to-Segment Gap Phasing*

Segment phasing is critical to achieving diffraction-limited performance. To achieve 500-nm diffraction-limited performance, the figure error of the primary mirror surface needs to be <10 nm rms. For a segmented mirror to achieve this specification, it is necessary to co-phase its mirror segments to <5 nm rms.

AMTD partner Harris Corp. designed, built, and characterized the "fine" stage of a low-mass two-stage actuator (Fig. 14), which could be used to co-phase mirror segments to the required tolerance. The "coarse" stage was previously demonstrated on a different project. Unfortunately, because of electronic noise, it was not possible to verify the actuator's predicted resolution.

Additionally, to avoid speckle noise, which can interfere with exoplanet observation, internal coronagraphs require a segment-to-segment dynamic co-phasing error of <10 pm rms between

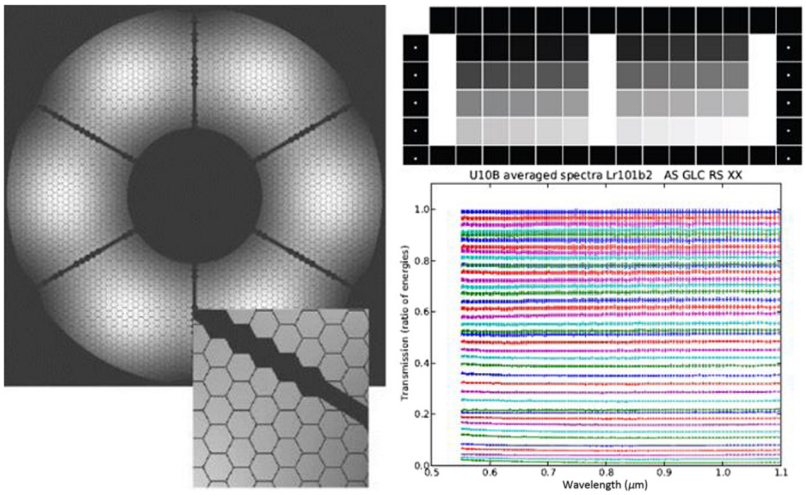

Fig. 13 Microdot apodization coating attenuation is flat as a function of wavelength.[41]

Property	Performance
Mass	0.313 Kg
Axial stiffness	40.9 N/μm
Test Range	14.1 μm
Resolution	6.6 nm (noise limited result) [expected is 0.8 nm]
Accuracy	1.1 μm

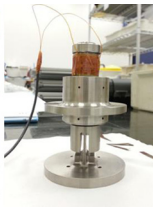

Fig. 14 Actuator and its performance test results.[2,30]

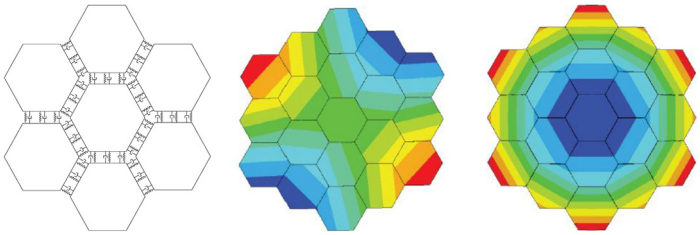

Fig. 15 Segmented mirror with edgewise interfaces can be tuned to have different bendings.

wavefront sensing and control updates. Although active phasing control at this level is beyond the scope of AMTD, two passive approaches were investigated.

First, AMTD investigated the utility of correlated magnetic interfaces to reduce the dynamic co-phasing error. Although it was found that such interfaces increase dampening by ~2×, they cannot achieve the required specification. It was also found that, while the correlated magnetic interfaces acted over a shorter distance than conventional magnets, their dampening was not significantly different from that provided by a conventional magnet. Therefore, given the inability of correlated magnetic interfaces to reduce dynamic segment-to-segment co-phasing error below the required level, investigation of this approach was stopped.

Next, AMTD co-investigator Jessica Gersh-Range conducted an analytical study that indicated that connecting segments at edges with damped spring interfaces provides potentially significant performance advantages for very large mirrors. With no edgewise connection, the segments behave independently. With as few as three damped spring interfaces, the segments start to act as a monolith (Fig. 15), provided that the interfaces are sufficiently stiff. Adjusting the spring stiffness tunes the assembly's first-mode frequency proportionally to the square root of the interface stiffness but approaches monolithic performance asymptotically. By adjusting the stiffness and damping, a segmented mirror will stabilize faster after a force impulse than a monolith. A segmented mirror with low to intermediate interface stiffness does not propagate disturbance waves, and a segmented mirror with high damping reduces the propagating wave amplitude quickly.[42–44]

5.6 *Integrated Model Validation*

On-orbit performance is driven by stability (both thermal and mechanical). As future systems become larger, compliance cannot be fully tested on the ground. Thus performance verification will rely on results from a combination of subscale tests and high-fidelity models. With never-before-required performance specifications, integrated STOP modeling of candidate PMAs (including substrates, structures, and mechanisms) and complete OTAs is critical to their design and performance modeling. To provide confidence that integrated STOP tools can design systems with never-before-required specifications, they must be validated by tests of full- and subscale components in relevant thermovacuum environments.

AMTD generated STOP models for the 1.5-m ULE® mirror (manufactured by AMTD partner Harris Corp.) and a 1.2-m Zerodur® mirror (owned by Schott North American). These models were used to predict the static and dynamic performance of each mirror, including: gravity sag, modal response, and thermal deformation.[38,45]

Both mirrors' thermal performances were characterized in the MSFC XRCF thermal-vacuum test chamber from 250 K to ambient. To enable testing of short-radius mirrors, a pressure-tight enclosure was built to place at the mirror's center of curvature: an interferometer to measure surface figure, an absolute distance meter to measure radius of curvature, and a thermal camera to measure front surface temperature distribution. The mirror and its mounting structure were extensively instrumented with temperature sensors (Fig. 16).[45]

Mechanical and thermal models were made of the Schott 1.2-m ELZM mirror. The mechanical model predicted a gravity sag deformation of 125 nm rms. The gravity sag measured via a rotation test was 142 nm rms (31 nm rms difference between predicted and measured), as shown in Fig. 17. Because the ELZM model was not an as-built model, this gravity sag difference could have been caused by a 2-mm error between the model and the actual mount pad locations. Thus

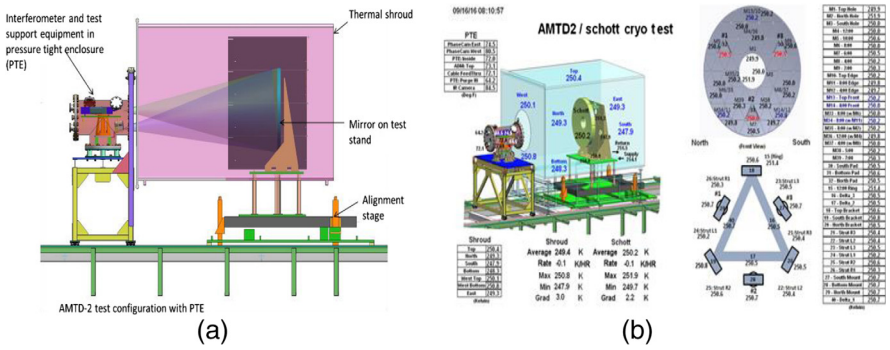

Fig. 16 (a) Short radius of curvature mirror test setup with pressure tight enclosure. (b) The test setup was extensively monitored via thermal sensors.

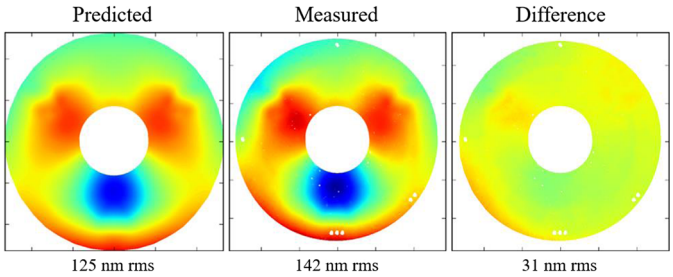

Fig. 17 ELZM gravity sag predicted versus measured.

a lesson learned, given the importance of gravity sag for achieving diffraction-limited performance, is the need for as-built mechanical models.

The mechanical model predicted a first free-free resonant bending mode of 207 Hz. ELZM first-mode frequency was measured via a roving tap test on foam blocks to be 196 Hz (5% agreement with prediction), shown in Fig. 18. The thermal model predicted a 9.6-nm rms total SFE consisting of contributions from its athermal mount through thickness thermal gradient and bulk CTE homogeneity. The largest contributor to this error is from an assumed CTE homogeneity of 5 ppb (based on internal Schott data). ELZM total thermal deformation measured from 294 to 250 K was 9.4 nm rms (Fig. 19).

Finally, a CTE homogeneity distribution estimate was created by correlating the model with the measured ELZM soak temperature thermal deformation. AMTD estimates that the Zerodur® boule from which the Schott 1.2-m mirror was manufactured had a slightly radial varying CTE distribution between 3.0 and 6.5 ppb/K (Fig. 20). With this CTE distribution, the thermal model predicts the measured thermal deformation with an uncertainty of <6 nm rms. Given the LTS induced core-wall bending experienced by the 1.5-m ULE® mirror, the team decided to make

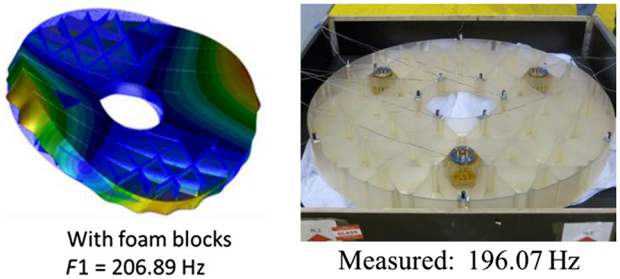

Fig. 18 ELZM first free-free modal frequency predicted versus measured.

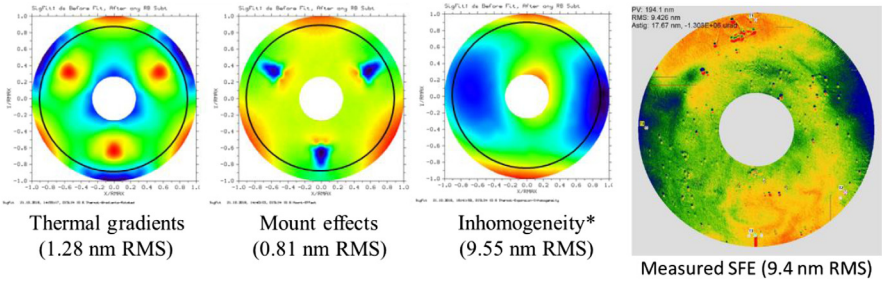

Fig. 19 ELZM thermal deformation predicted versus measured.[38]

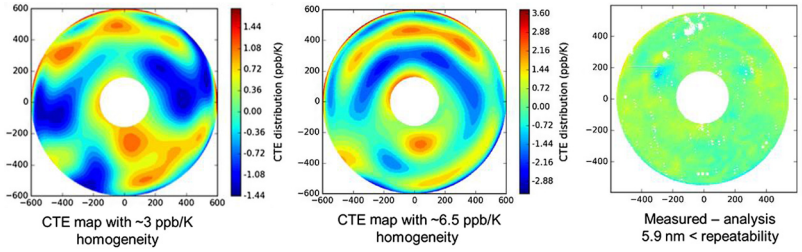

Fig. 20 ELZM estimated CTE distribution from measured thermal deformation.[38]

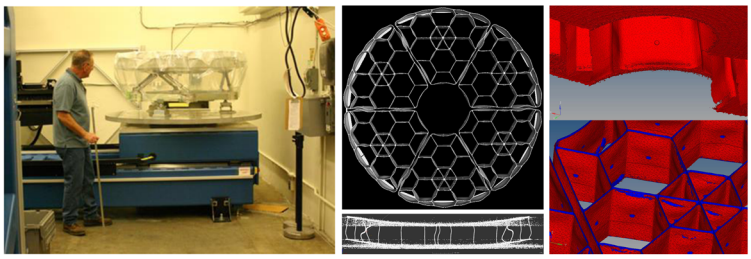

Fig. 21 Internal dimensional structure of the 1.5-m AMTD-2 mirror was quantified via x-ray-computed tomography, and code was developed by MSFC to convert CT scan data into a finite-element model.

an as-built model of its internal structure via x-ray tomography (Fig. 21). This model was used to predict the mechanical and thermal performance of the 1.5-m ULE® mirror.

The MSFC as-built mechanical model predicted a gravity sag deformation of 2.5 μm pv (580 nm rms). The gravity sag measured via a rotation test was 2.6 μm pv (582 nm rms, a 55-nm rms difference between predicted and measured), as shown in Fig. 22. By comparison, the Harris Corp. "design" model predicted a 3.0-μm pv (681 nm rms). The as-built mirror is stiffer than its design. This is because, during mirror assembly, due to a fixture issue from an external vendor, some of the hex core elements were shifted radially inward from their design location by up to 20 mm. In addition to producing a stiffer mirror, it decreased the gap between adjacent core elements and may have contributed to core-wall contact due to bending during slumping.

When the ELZM mirror was tap tested resting on foam, the 1.5-m ULE® mirror and its support structure were tested suspended from a bungee. The mirror and structure were tapped at 42 locations with an instrumented modal test hammer. Each location was tapped 5 times, and results were averaged. Twenty-two of the 42 locations were on the back of the ULE® mirror. Test results were deciphered to identify the modes associated with the ULE® mirror. Those results were

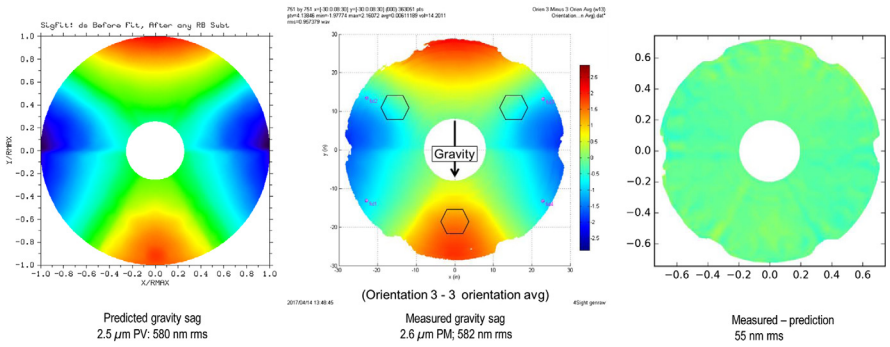

Fig. 22 1.5-m ULE® mirror gravity sag predicted versus measured.

As-built FEM frequency (Hz)	Design FEM frequency (Hz)	Measured frequency (Hz)	Difference (%)	Test damping (%)	As-built FEM mode shape
400.8 401.9	395.4 398.9	414.4 417.2	3.3 3.7	0.31 0.49	
673.1	646.1	678.7	0.8	0.59	
705.7	682.4	707.5	0.3	0.32	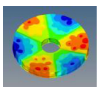
835.5 843.9	834.0 834.8	864.1 868.9	3.3 2.9	0.46 0.41	
866.1	861.4	877.4	1.3	0.42	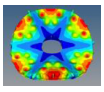

Fig. 23 Predicted versus measured modal frequencies of 1.5-m ULE® mirror.[46]

compared to predicted frequencies from the MSFC as-built model and the Harris Corp. design model (Fig. 23). Again, the as-built model is stiffer than the design model and more closely matches the test data. The as-built model predicted a first mode of 401 Hz, and the measured first mode was 414 Hz (3.3% agreement).[46]

The 1.5-m ULE® mirror thermal model was constructed by combining the x-ray computed tomography structure data, boule CTE maps provided by Harris Corp., and an MSFC CTE homogeneity correlation. The model was used to correlate the mirror's estimated performance with its "as-measured" performance (Fig. 24). The measured thermal surface change (231 to

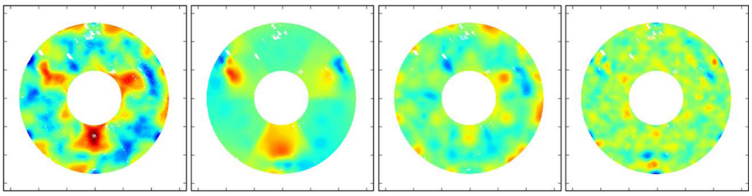

Fig. 24 1.5-m ULE® mirror thermal deformation predicted versus measured.[38]

293 K) was 28.8 nm rms. The model estimated that the mirror would have 18.9 nm rms of mount deformation (caused by CTE of the aluminum delta frame relative) and 16.6 nm rms of CTE deformation (caused by ULE® CTE distribution and homogeneity), for a total SFE of 22.8 nm rms. The difference was 13.4 nm rms. One explanation for the 13.4-nm-rms residual is uncertainty in the best-fit CTE homogeneity correlation. Another potential explanation is differential strain between the front and back face sheets. Introducing such an effect into the model by adding a uniform bias to the back sheet CTE reduced the uncorrelated error to 4.4 nm rms. However, it must be noted that at present we have no physical basis for how such a differential strain could arise.

6 TRL Assessment

At the start of AMTD, the AMTD team assessed 4-m class monolithic UVOIR space mirrors to be TRL-3. This assessment was based on the existence of multiple subscale mirrors including Hubble at 2.4 m, Kepler at 1.4 m, AMSD at 1.5 m, and WFIRST at 2.4 m. The AMTD team proposed advancing 4-m monolithic UVOIR mirrors to TRL-4 by maturing three key technologies: deep substrates, support system, and mid/high-spatial error. Between November 2014 and February 2015, an independent COR Program Office Technology Management Board (TMB) assessed AMTD. The TMB found that (1) "larger aperture (≥4 m-diameter), low-areal density, high-stiffness mirror substrate development is currently at TRL-3" and (2) if successfully completed, AMTD "will elevate the flat-to-flat stacked-core ULE® mirror substrate technology to TRL-4."

AMTD assesses that, with varying degrees of success, it matured each of its identified six critical technologies, documented its lessons learned, and identified new areas of investigation necessary to enable large monolithic or segmented ultrastable UVOIR space telescopes. Table 6 summarizes the AMTD Team's assessment of current TRL.

For the key technology of large-aperture stiff substrates, AMTD successfully demonstrated the utility of stacked-core technology to enable ultrastiff/ultrastable mirrors. Three specific abilities were demonstrated: the ability to LTF stack-cores with strength greater than the design allowable limit, the ability to make mirror substrates as thick as 40 cm, and the ability to laterally scale the stacked-core technique to 1.5 m. Additionally, both the 43-cm and 1.5-m mirrors were tested in a relevant thermal environment. The ability to low-temperature slump a 1.5-m class substrate into an F/1.25 mirror was not successfully demonstrated.

For the key technology of support systems, AMTD advanced the state of the art by developing modeling software that integrates the design and analysis of the mirror structure and support structure. Additionally, AMTD characterized the performance of a flight-like mirror/strut bond pad interface traceable to the WFIRST program.

For mid-spatial frequency error, AMTD partner Harris Corp. demonstrated on the 43-cm mirror the ability to correct quilting errors to better than 6 nm rms surface. The AMTD project assesses this capability to be mature at TRL-6.

For segment edges, AMTD Partner Space Telescope Science Institute tested in a laboratory environment an achromatic-attenuation microdot coating technology for edge apodization.

Regarding segment-to-segment gap phasing, possibly AMTD's most important result was deriving, from science requirements, the 10-pm per control cycle co-phasing specification. Unfortunately, when segmented telescopes have been phased for infrared diffraction-limited performance, no existing segmented telescope has ever achieved 10-pm stability—not even in a laboratory environment.

Although the COR Program Office TMB did not define integrated modeling as a technology, a major focus of AMTD was developing integrated modeling tools and validating those tools. Two important advances were (1) using x-ray-computed tomography to create a high-fidelity mapping of the mirror's internal structure and (2) determining CTE homogeneity via cryogenic test. These two new technology advances enhance the fidelity of STOP analysis by helping correlate predicted performance with the mirror's as-built conditions. The AMTD TRL assessment is provided in Table 6.

Table 6 AMTD TRL assessment.

Technology	Assessed TRL	Basis of assessment
4-m diameter × 40-cm-thick ultrastable mirror substrates	TRL 5	AMTD demonstrated stacked-core assembly of thick mirrors via LTF on two 5-layer subscale mirrors and tested them in a relevant thermal environment: • 43 cm × 400 mm (depth demonstration) • 1.5 m × 165 mm (lateral demonstration)
LTS of thick substrate to *F*/1.25	TRL 4	• LTS of thin 1.5-m mirrors demonstrated in a relevant environment via AMSD • LTS of thick mirrors demonstrated on AMTD 43-cm mirror in a relevant thermal environment • LTS of thick F/1.25 mirrors demonstrated on AMTD 1.5-m mirror in a laboratory environment • However, design parameters prevented it from achieving its performance specification in a relevant environment
Support system	TRL 5	• Modeling software fully capable of including integrated support structure. Limitation is property knowledge support materials, particularly thermal properties • A "flight" like mirror strut bonding pad traceable to WFIRST was characterized in a relevant environment
<6 nm rms mid/high-spatial frequency error	TRL 6	• Demonstrated <6 nm rms surface on AMTD 43-cm mirror in a relevant thermal environment with no quilting error
Segment edge apodization	TRL 3	• Achromatic attenuation of microdot apodization coating demonstrated in a laboratory environment
Segment gap phasing	TRL 2	• Co-phasing specification to enable coronagraphy application has been defined • No proof of concept exists. No existing segmented telescope or laboratory experiment has ever demonstrated 10-picometer per 10-min stability
Mechanical modeling	TRL 5	• AMM rapid model development enables optimal solutions by parametrically evaluating mirror configurations, core designs, and support systems • X-ray computed tomography enables high-fidelity as-built mechanical models that improve STOP analysis
Thermal modeling	TRL 5	• Characterized 1.2-m Zerodur® and 1.5-m ULE® mirrors in a relevant thermal environment • Predicted thermal deformations

7 Conclusions

The AMTD project was a 6-year effort to mature critical technologies required to enable 4-m-or-larger monolithic or segmented UVOIR space telescope primary mirror assemblies. AMTD used a science-driven systems-engineering approach to derive engineering specifications from science requirements. Potentially the most impactful of these may be the "poetic" 10 pm per 10-min wavefront stability specification. Advances were made to six key technologies: (1) fabricating large-aperture low-areal-density high-stiffness mirror substrates; (2) designing support systems; (3) correcting mid/high-spatial frequency figure error; (4) mitigating segment edge diffraction; (5) phasing segment-to-segment gaps; and (6) validating integrated models.

AMTD successfully demonstrated the utility of stacked-core technology to enable ultrastiff/ultrastable substrates. AMTD partner Harris Corp. accomplished this by demonstrating three specific capabilities: (1) the ability to LTF stack-cores with strength greater than the design allowable limit, (2) the ability to make mirror substrates as thick as 40 cm, and (3) the ability to laterally scale the stacked core technique to a 1.5-m diameter by 165-mm-thick, 450-Hz mirror (1/3 scale of a 4-m mirror). Additionally, lessons were learned regarding the need to design mirror core elements to manage stress during LTS.

AMTD evaluated multiple PMA designs (substrate and mount system) using the AMM tool, which rapidly creates and analyzes detailed mirror designs. Candidate mirror systems were evaluated for their stiffness, mass, static, and dynamic performance deformations and their ability to survive launch loads. Specific design trades examined include closed-back versus open-back, flat-back versus meniscus substrates, core dimensions, mount location, and pad size and location.

AMTD advanced the maturity of mid-spatial frequency WFE by demonstrating the impact of core cell size versus pocketed face sheets on print through figure error and the ability to correct mid-spatial error. But, the more important lesson may be the importance of CTE homogeneity on mid-spatial frequency error. To achieve the required wavefront stability for coronagraphy, the primary mirror system either must have extremely good CTE homogeneity (<5 ppb/K) or must be actively controlled to an extremely stable temperature (<10 mK).

AMTD phase 1 investigated two specific segmented mirror technologies. AMTD partner STScI successfully demonstrated an achromatic apodization coating. A glass grayscale prototype mask was fabricated using chromium microdots and tested at the Brookhaven National Laboratory beam line. AMTD partner Harris Corp. designed, built, and characterized the "fine" stage of a low-mass two-stage actuator, which could be used to co-phase mirror segments to <5 nm rms. AMTD also investigated, with limited success, methods to minimize dynamic segment-to-segment co-phasing error—the bottom line is that this is an extremely complex problem.

Finally, for help predicting on-orbit performance and assisting in architecture trade studies, integrated models were created for two mirror assemblies (1.5-m ULE® mirror fabricated by AMTD partner Harris Corp. and 1.2-m Zerodur® mirror owned by Schott North American). X-ray-computed tomography was used to construct the 1.5-m ULE® mirror's as-built model. These models were validated by test in a relevant thermovacuum environment at MSFC.

8 Appendix: Modeling Tools

AMTD developed four modeling tools to assist in STOP analysis trade studies of candidate primary mirror assemblies (including substrates, structures, and mechanisms) and complete OTAs: AMM, SPECL, T-MTF, and FaRSiTe.

8.1 *Arnold Mirror Modeler*

The AMM was developed to rapidly create and analyze detailed mirror designs. AMM can create a 400,000-element model in minutes. This tool facilitates the transfer of a high-resolution mesh to various mechanical and thermal analysis tools. AMM creates input decks for ANSYS, ABAQUS, and NASTRAN. It creates a complete analysis stream, including model, loads (static and dynamic), plots, and a summary file of input variables and results suitable for optimization or trade studies. The values of all settings in the program are archived and recalled to continue or redo any configuration. AMM supports a range of mirror architectures:

- monolithic (circular and elliptical—with or without center hole);
- segmented (hex and petal);
- on- and off-axis;
- open- and closed-back;
- hex-grid and iso-grid core structures;
- shaped-back designs (SOFIA, T-ribs, etc.);
- strut designs (hexapod, Hindle, axial, radial, tangent, etc.);
- automatic support pad positioning;
- launch support systems.

Supported strut configurations include hexapod, Hindle, axial, radial, and tangential. Struts can either follow the contour of the mirror to attach to a curved backplane or have variable length for attachment to a flat backplane (Fig. 25). For large segmented mirrors, AMTD used the curved backplane option. This provides more uniform strut stiffness for dynamic behavior. For ease of

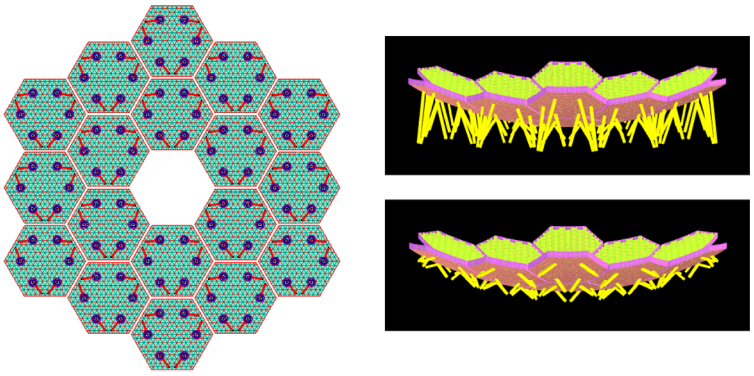

Fig. 25 Hexapod support system for large aperture—flat versus curved backplane.

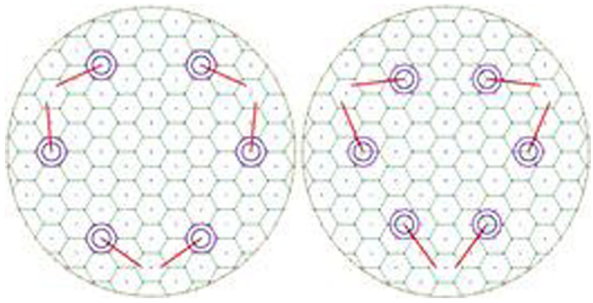

Fig. 26 Algorithm locates mount pads at cell center or rib intersections.

design, an algorithm aligns the mount pads to either the center of a cell or the intersection of cell webs (Fig. 26).

8.2 *Sensitivity and Performance Evaluator for Coronagraph Leakage*

AMTD developed a series of increasingly sophisticated modeling tools to estimate the contrast leakage that occurs when dynamically aberrated wavefronts are propagated through candidate coronagraphs.[18,22,23] The purpose of these tools is to help define a wavefront stability specification for candidate primary mirror architectures. The SPECL tool has the ability to study monolithic, hex segmented, and petal segmented primary mirror architectures (Fig. 27). It can apply global Seidel aberrations upon the whole aperture of power, astigmatism, coma, spherical, etc., or it can apply Zernike aberrations to individual segments, including piston and tip/tilt. It also models the effect of backplane bending on a segmented aperture. For each of these cases, it can introduce an error that is static, periodic, or randomly varying. Static errors determine the sensitivity of a coronagraph to a fixed amplitude of each aberration. Periodic models contrast leakage for a WFE that varies sinusoidally between $\pm$peak amplitude values. This case represents periodic vibration, such as the rocking mode of a secondary mirror tower or of a primary mirror segment that is uncorrected (either no active control or active control is slow). Random models motion is not corrected by an assumed active control system. Following the definitions and methodology of Shaklan,[47] the contrast leakage is decomposed into radial (photonic noise) and azimuthal (systematic noise) components. Contrast leakage is calculated over an annual region of interest (ROI) and plotted as a function of aberration type and amplitude (Fig. 28).[22,23]

8.3 *Thermal MTF*

AMTD developed a methodology for understanding how a primary mirror responds to a dynamic thermal environment.[19] Any thermal environment can be decomposed into a set of

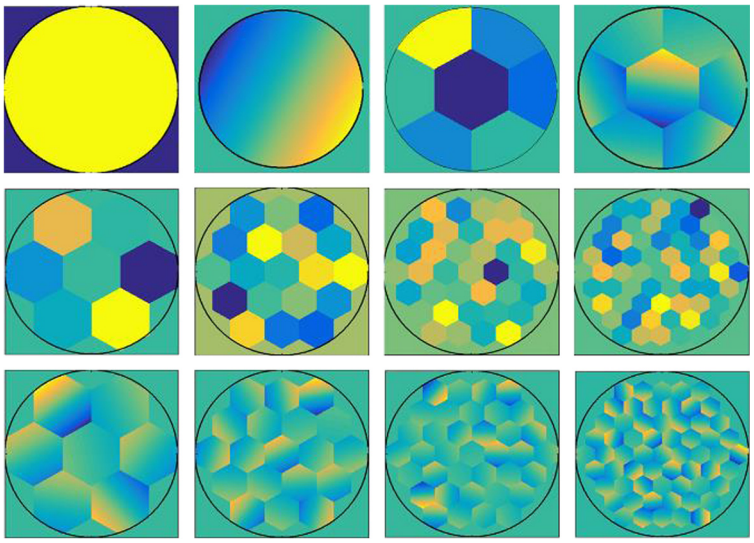

Fig. 27 SPECL supports various apertures: monolithic and segmented (petal and hex).[4,22]

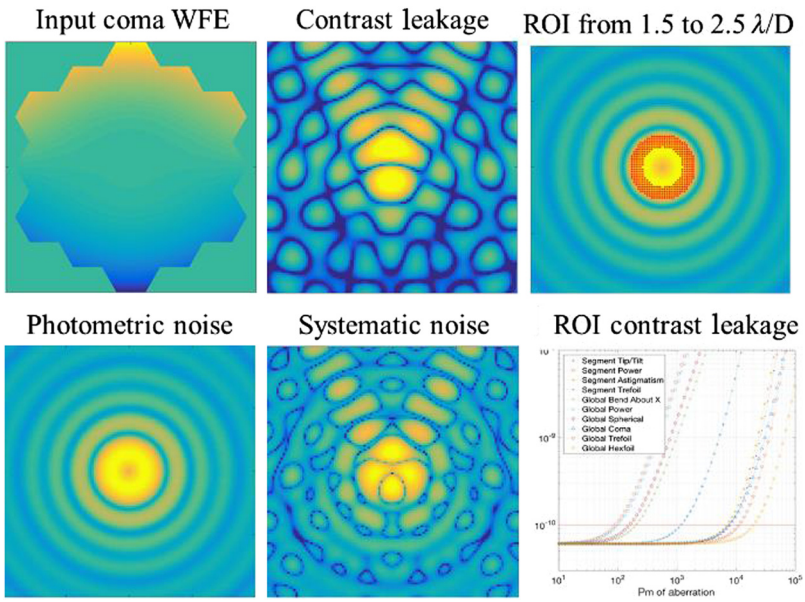

Fig. 28 SPECL calculates contrast leakage over annular ROI as function of aberration.[23]

periodic thermal oscillations that cause wavefront figure errors on the primary mirror with a thermal time constant determined by the mirror's thermal properties (e.g., mass and conductivity), as shown in Fig. 29. The magnitude of these figure errors depends on the amplitude and period of the input thermal oscillation. These T-MTF responses can be used to determine thermal boundary and control conditions for passive and active telescope thermal control.

Integrated modeling shows that the RMS WFE range is inversely proportional to the mirror's mass and specific heat and the RMS WFE range is linearly proportional to the mirror's CTE. A closed-form derivation found similar relationships between thermal parameters and the thermal strain rate caused by a heat imbalance:

$$\frac{\mathrm{d}L}{\mathrm{d}t} = \frac{(\mathrm{CTE})L}{V\rho c_p}\frac{\mathrm{d}Q}{\mathrm{d}t}.$$

Based on these findings, two figures of merit for thermally stable mirror materials are defined as follows:

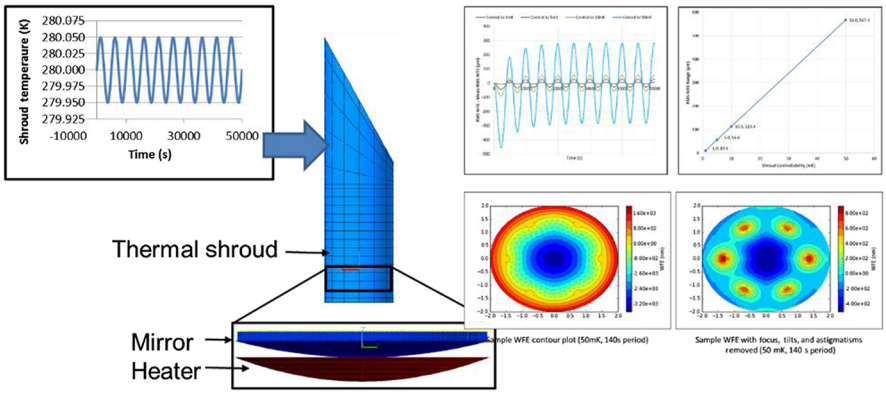

Fig. 29 Primary Mirror optical performance depends the mirror's response to thermal modulation as a function temporal frequency.

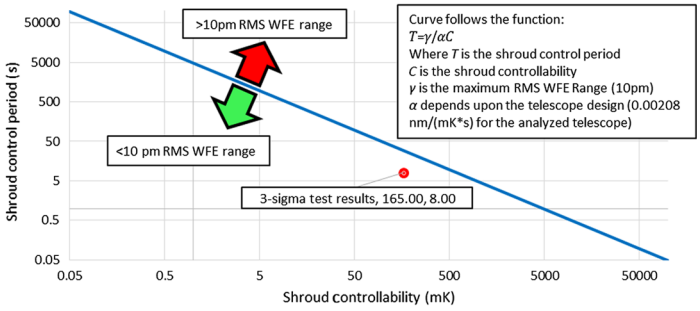

Fig. 30 For a given telescope, its wavefront stability can be kept below a specified value by varying shroud controllability and cycle period.

$$\text{massive active optothermal stability (MAOS)} = \frac{c_p \rho}{\text{CTE}},$$

and

$$\text{active opto thermal stability (AOS)} = \frac{c_p}{\text{CTE}}.$$

Selecting a mirror substrate with higher MAOS and AOS will result in a lower thermal strain rate in the mirror (i.e., a slower WFE change rate).

AMTD explored telescope thermal stability sensitivity for candidate 4-m-class mirrors. The required WFE stability can be achieved when the primary mirror is inside a thermally controlled environment with a period and controllability that meet the specifications shown in Fig. 30. Controllability is the maximum deviation of the shroud's temperature from the average temperature. The period of the control system is the time it takes for an entire heater cycle to occur.

8.4 *Fast Response Simulator for Telescopes*

From FY11 to FY13, AMTD partner GSFC developed a suite of MATLAB®-based tools for using STOP and jitter-integrated models to calculate optical path length difference maps and line-of-sight errors called FaRSiTe (Fig. 31).[2] FaRSitE can be used to generate high-fidelity PSF simulations and compute standard metrics associated with imaging systems (MTF, EE, Zernike coefficients, etc.), as well as user-defined metrics. This represents an advance over the previous state of the art in which performance estimates from multiple independent sources were often combined via an error budget framework (e.g., via root-sum-squares of scalar quantities, where all terms are assumed to be independent whether this is actually the case or not).

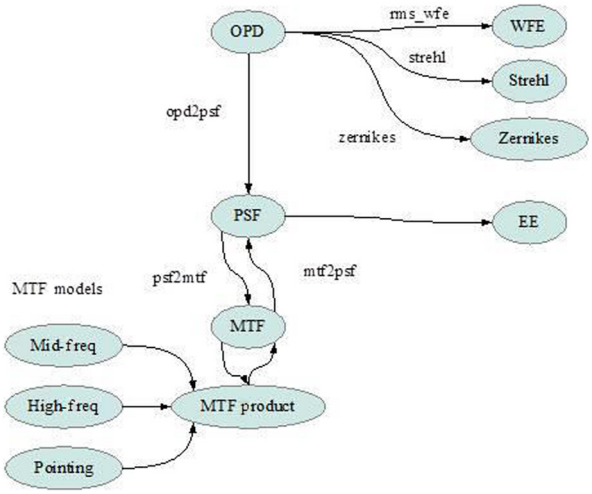

Fig. 31 Fast Response Simulator for Telescopes.

Acknowledgments

The Science team was chaired by Dr. Marc Postman of the Space Telescope Science Institute and consisted of (in alphabetical order): Dr. Olivier Guyon, University of Arizona; Dr. John E. Krist, Jet Propulsion Laboratory; Dr. Bruce A. Macintosh, Lawrence Livermore National Laboratory; Dr. Anand Sivaramakrishnan, Space Telescope Science Institute; Dr. Remi Soummer, Space Telescope Science Institute; and Dr. Christopher Stark, Space Telescope Science Institute. The Engineering team was chaired by Dr. H. Philip Stahl of NASA Marshall Space Flight Center (MSFC) and consisted of engineers from NASA (in alphabetical order), followed by partners' personnel: William Arnold, NASA MSFC Contractor; Carl Blaurock, NASA Goddard Space Flight Center (GSFC) Contractor; Thomas Brooks, NASA MSFC; Jacqueline Davis, NASA MSFC; Ron Eng, NASA MSFC; Kong Ha, NASA GSFC; Brent Knight, NASA MSFC; David Lehner, NASA MSFC (Ret.); Gary Mosier, NASA GSFC; Stuart Shaklan, Jet Propulsion Laboratory (JPL); W. Scott Smith, NASA MSFC; Mark Stahl, NASA MSFC; Laura Abplanalp, Harris Corp.; Robert Egerman, Harris Corp.; Gary W. Matthews, Harris Corp.; Steven P. Maffett, Harris Corp.; and Tony Hull, Schott. Finally, AMTD benefited from the involvement of multiple students: Jessica Gersh-Range, Cornell University; Hao Tang, University of Michigan (2018); Jonathan Gaskins, University of North Carolina at Charlotte (2017); Mary Cobb, University of Alabama in Huntsville (UAH) (2017); Nathaniel Stepp, UAH (2016); Marshall Prince, Texas A&M (2016); Jacob Vehonsky, Arizona State University (2015); James Holt, West Texas A&M University (2014); Jeremy Haibach, University of Alabama (2014); Ryan Bevan, UAH (2013, 2012); Erik Humfleet, Miami University (2013); Amanda Smith, Wichita State University (2013); Ruben Jaca, University of Puerto Rico Mayaguez (2013); Matthew Fitzgerald, University of Tennessee Martin (2012); Brian Newman, University of Florida (2012, 2011); and Matthew Pugh, University of Alabama (2012).

References

1. H. P. Stahl et al., "Overview and recent Accomplishments of the Advanced Mirror Technology Development (AMTD) for large aperture UVOIR space telescopes project," *Proc. SPIE* **8860**, 88600Q (2013).
2. H. P. Stahl et al., "Advanced Mirror Technology Development (AMTD) project: 2.5 year status," *Proc. SPIE* **9143**, 91431S (2014).
3. H. P. Stahl, "Overview and accomplishments of Advanced Mirror Technology Development Phase 2 (AMTD-2) project," *Proc. SPIE* **9602**, 960208 (2015).
4. H. P. Stahl, "Advanced Mirror Technology Development (AMTD) project: overview and year four accomplishments," *Proc. SPIE* **9912**, 99120S (2016).

5. H. P. Stahl, "Advanced Mirror Technology Development (AMTD): year five status," *Proc. SPIE* **10401**, 104010O (2017).
6. H. P. Stahl, *Advanced UVOIR Mirror Technology Development for Very Large Space Telescopes*, NASA, Marshall Space Flight Center, Huntsville, Alabama
7. National Research Council, *New Worlds, New Horizons in Astronomy and Astrophysics*, p. 324, The National Academies Press, Washington, D.C. (2010).
8. National Research Council, *NASA Space Technology Roadmaps and Priorities: Restoring NASA's Technological Edge and Paving the Way for a New Era in Space*, p. 376, The National Academies Press, Washington, D.C. (2012).
9. C. Kouveliotou et al., *Enduring Quests, Daring Visions: NASA Astrophysics in the Next Three Decades*, p. 110 (2014).
10. P. Hertz, "*2020 decadal survey planning*," 2015, https://science.nasa.gov/astrophysics/2020-decadal-survey-planning
11. J. Dalcanton et al., *From Cosmic Birth to Living Earths: The Future of UVOIR Space Astronomy*, Association of Universities for Research in Astronomy, Washington, D.C., www.hdstvision.org/report/ (2015).
12. M. S. Lake, L. D. Peterson, and M. B. Levine, "Rationale for defining structural requirements for large space telescopes," *J. Spacecr. Rockets* **39**(5), 674–681 (2002).
13. H. P. Stahl et al., "Summary of the NASA science instrument, observatory, and sensor system (SIOSS) technology assessment," *Proc. SPIE* **8146**, 81460C (2011).
14. H. P. Stahl, M. Postman, and W. S. Smith, "Engineering specifications for large aperture UVO space telescopes derived from science requirements," *Proc. SPIE* **8860**, 886006 (2013).
15. H. P. Stahl et al., "AMTD: update of engineering specifications derived from science requirements for future UVOIR space telescopes," *Proc. SPIE* **9143**, 91431T (2014).
16. W. R. Arnold et al., "Next generation lightweight mirror modeling software," *Proc. SPIE* **8836**, 88360I (2013).
17. W. R. Arnold, "Recent updates to the Arnold Mirror Modeler and integration into the evolving NASA overall design system for large space-based optical systems," *Proc. SPIE* **9573**, 95730H (2015).
18. B. Nemati et al., "HabEx Telescope WFE stability specification derived from coronagraph starlight leakage," *Proc. SPIE* **10743**, 107430G (2018).
19. T. Brooks, H. P. Stahl, and W. R. Arnold, "Advanced Mirror Technology Development (AMTD) thermal trade studies," *Proc. SPIE* **9577**, 957703 (2015).
20. H. P. Stahl, "JWST mirror technology development results," *Proc. SPIE* **6671**, 667102 (2007).
21. H. P. Stahl, "JWST primary mirror technology development lessons learned," *Proc. SPIE* **7796**, 779604 (2010).
22. M. T. Stahl, H. P. Stahl, and S. B. Shaklan, "Preliminary analysis of effect of random segment errors on coronagraph performance," *Proc. SPIE* **9605**, 96050P (2015).
23. M. T. Stahl, H. P. Stahl, and S. B. Shaklan, "Contrast leakage as a function of telescope motion," in *Mirror Technology Days* (2016).
24. B. Nemati et al., "Effects of space telescope primary mirror segment errors on coronagraph instrument performance," *Proc. SPIE* **10398**, 103980G (2017).
25. H. P. Stahl et al., "Designing astrophysics missions for NASA's Space Launch System," *J. Astron. Telesc. Instrum. Syst.* **2**(4), 041213 (2016).
26. M. N'Diaye et al., "Apodized pupil lyot coronagraphs for arbitrary apertures," *Astrophys. J. Lett.* **618**, L161–L164 (2016).
27. G. W. Matthews et al., "The development of stacked core technology for the fabrication of deep lightweight UV-quality space mirrors," *Proc. SPIE* **8838**, 88380L (2013).
28. G. W. Matthews et al., "Processing of a stacked core mirror for UV applications," *Proc. SPIE* **8837**, 88370A (2013).
29. R. Egerman et al., "Status of the Advanced Mirror Technology Development (AMTD) phase 2 1.5m ULE mirror," *Proc. SPIE* **9575**, 95750L (2015).
30. R. Egerman, *AMTD Final Report*, Harris Corporation, Melbourne, Florida (2018).

31. W. R. Arnold, "Evolving design criteria for very large aperture space-based telescopes and their influence on the need for intergrated tools in the optimization process," *Proc. SPIE* **9573**, 95730G (2015).
32. W. R. Arnold and H. P. Stahl, "Design trade study for a 4-meter off-axis primary mirror substrate and mount for the Habitable-zone Exoplanet Direct Imaging Mission," *Proc. SPIE* **10398**, 1039808 (2017).
33. W. R. Arnold, R. M. Bevan, and H. P. Stahl, "Integration of mirror design with suspension system using NASA's new mirror modeling software," *Proc. SPIE* **8836**, 88360J (2013).
34. W. R. Arnold and H. P. Stahl, "Influence of core and hexapod geometry, and local reinforcement on the performance of ultra lightweight ULE mirror," *Proc. SPIE* **10743**, 107430B (2018).
35. J. M. Davis et al., "HabEx primary mirror trade studies," *Proc. SPIE* **10371**, 103710B (2017).
36. R. Eng et al., "Cryogenic optical performance of a lightweighted mirror assembly for future space astronomical telescopes: correlating optical test results and thermal optical model," *Proc. SPIE* **8837**, 88370B (2013).
37. G. Matthews, et al., "Thermal testing of a stacked core mirror for UV applications," in presented at *SPIE Conf. Mater. Technol. and Appl. to Opt., Struct. Comp. and Sub-Syst.*, NASA, Marshall Space Flight Center, Huntsville, Albama (2013).
38. T. E. Brooks et al., "Optothermal stability of large ULE and Zerodur mirrors," *Proc. SPIE* **10743**, 107430A (2018).
39. N. Yaitskova, K. Dohlen, and P. Dierickx, "Analytical study of diffraction effects in extremely large segmented telescopes," *J. Opt. Soc. Am. A* **20**(8), 1563–1575 (2003).
40. N. Yaitskova and M. Troy, "Rolled edges and phasing of segmented telescopes," *Appl. Opt.* **50**(4), 542–553 (2011).
41. A. Sivaramakrishnan et al., "Calibrating apodizer fabrication techniques for high contrast coronagraphs on segmented and monolithic space telescopes," *Proc. SPIE* **8860**, 88600W (2013).
42. J. Gersh-Range, "Design, control, and failure mitigation for segmented space telescopes," Ph.D. Dissertation, Mechanical Engineering, Cornell University (2014).
43. J. Gersh-Range, W. R. Arnold, and H. P. Stahl, "Edgewise connectivity: an approach to improving segmented primary mirror performance," *J. Astron. Telesc. Instrum. Syst.* **1**(1), 014002 (2014).
44. J. Gersh-Range et al., "Flux-pinning mechanisms for improving cryogenic segmented mirror performance," *J. Astron. Telesc. Instrum. Syst.* **1**(1), 014001 (2014).
45. T. E. Brooks et al., "Modeling the Extremely Lightweight Zerodur Mirror (ELZM) thermal soak test," *Proc. SPIE* **10374**, 103740E (2017).
46. J. B. Knight et al., "Advanced Mirror Technology Development (AMTD) II modal test of a 1.5 m ultra low expansion slumped mirror," *Proc. SPIE* **10742**, 1074203 (2018).
47. S. B. Shaklan et al., "Stability error budget for an aggressive coronagraph on a 3.8 m telescope," *Proc. SPIE* **8151**, 815109 (2011).

H. Philip Stahl received his PhD in optical science from the University of Arizona in 1985. He is a senior optical physicist at NASA MSFC. He is a leading authority in optical systems engineering, metrology, and phase-measuring interferometry. He is developing technology and processes to design, manufacture, and test ultrastable, high-precision space telescopes, such as HabEx. Previous assignments include Mirror Technology Lead for the Webb telescope. He is a fellow of SPIE and OSA and was the SPIE 2014 President.